Molecular Crystals and Liquid Crystals
Publication details, including instructions for authors and subscription information:
http://www.tandfonline.com/loi/gmcl16

Optical Studies on Williams Domains

D. Krishnamurti [a] & D. Revannasiddaiah [a]
[a] Department of Physics, University of Mysore, Mysore, 570 006, India
Version of record first published: 14 Oct 2011.

To cite this article: D. Krishnamurti & D. Revannasiddaiah (1979): Optical Studies on Williams Domains, Molecular Crystals and Liquid Crystals, 55:1, 33-46

To link to this article: http://dx.doi.org/10.1080/00268947908069788

Mol. Cryst. Liq. Cryst., 1979, Vol. 55, pp. 33–46
0026-8941/79/5501-0033$04.50/0

Printed in United States of America

Optical Studies on Williams Domains

D. KRISHNAMURTI and D. REVANNASIDDAIAH
Department of Physics, University of Mysore, Mysore 570 006, India

(*Received March 13, 1979*)

The paper discusses the interference studies carried out on Williams domains in the case of *N*-(*p*-propoxybenzylidene) *p*-pentylaniline. Measurements of the periodic variation of the orientation of the director in the nematic medium are reported.

1 INTRODUCTION

It is well-known that when an oriented nematic material with negative dielectric anisotropy is placed between two transparent conducting electrodes and when a dc or an alternating voltage of the order of a few volts (above a critical threshold) is applied, distortions in the molecular orientation take place giving rise to optical effects.[1–5] When the specimen is examined under the polarizing microscope with the vibration direction of the polarizer parallel to the original direction of the orientation of the specimen by rubbing, series of alternating bright and dark areas are observed, giving the impression of a series of parallel "stripes" and these are referred to as "Williams domains." The stripes are perpendicular to the original direction of molecular orientation, i.e. the director **S**. If the vibration direction of the incident light is perpendicular to that of the rubbing direction, the pattern of stripes disappears.

The spacing of the stripes is of the order of 10 μm and it had been observed[6–10] that the Williams domains can act as diffraction gratings, giving rise to several orders of diffraction spectra. Figures 1(a) and 1(b) show respectively the typical stripes of the Williams domains and the diffraction spectra exhibited by *N*-(*p*-propoxybenzylidene)*p*-pentylaniline (PBPA). The origin of the stripes and the polarization effect referred to above have been

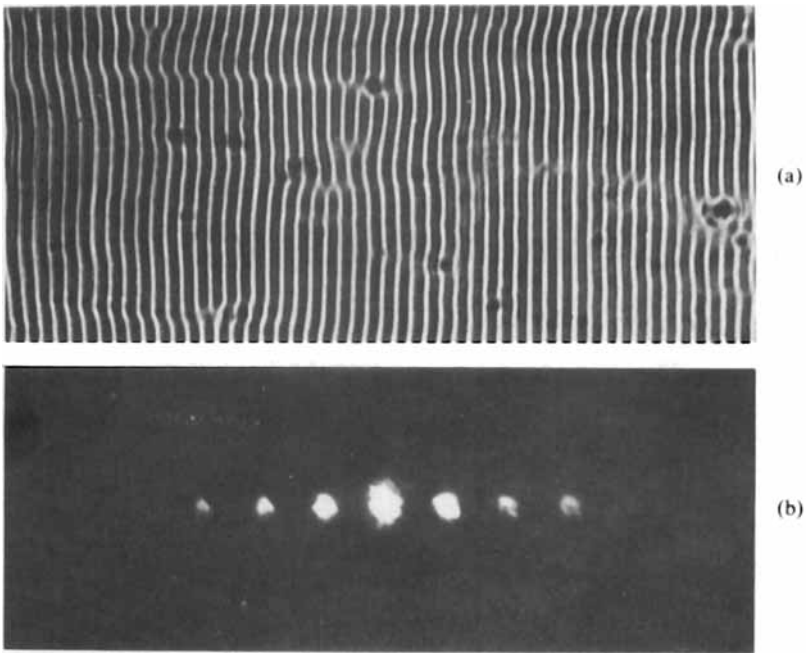

FIGURE 1 (a) Enlargement of the Williams domain pattern, obtained with a specimen of thickness 18.45 μm to which an alternating voltage of 23.5 V, (1000 Hz) was applied. The spacing between the stripes is equal to 18 μm. (b) Diffraction pattern obtained with the Williams domains shown in Figure 1(a), using unpolarized light of wavelength 5893 Å.

explained on the basis of periodic distortions of the original nematic alignment. Here, the long axes of the molecules undergo a periodic change in the orientation as shown in Figure 2(a). The striped pattern arises as a consequence of the periodic variation of the local extraordinary refractive index and the associated cylindrical lens-like focusing effect, (see for example, Penz).[11]

The present paper reports the results of our optical studies carried out with a view to estimate the extent of the periodic distortions in the molecular orientation in Williams domains.

2 EXPERIMENTAL

In a recent paper[12] we have discussed and confirmed the helicoidal nature of the molecular orientation in the case of ringed spherulites with the aid of two sensitive optical interference methods. In the present investigation we have made use of the same experimental methods to study quantitatively the

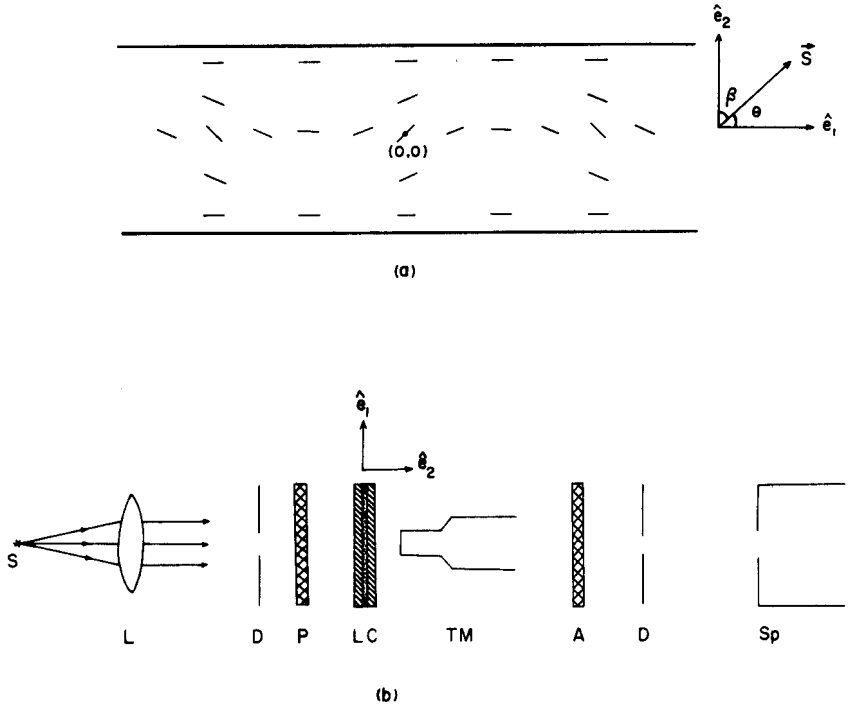

FIGURE 2 (a) The orientation of rod-like molecules in Williams domains. Incident light is along $\hat{e}_2$. (b) Plan view of the experimental arrangement: S = light source; L = lens; D = apertures; P = polarizer at 45° to vertical; LC = nematic sample sandwiched between two conducting glass plates; TM = travelling microscope; A = analyzer (crossed with polarizer); Sp = spectrograph.

periodic variation of the molecular orientation in Williams domains. At first the experimental method involving the banded spectrum is summarized in the following.

When white light transmitted by a birefringent material kept between crossed polars, is examined with a spectroscope, the spectrum of the emergent light is found to be traversed by a series of dark bands. When the principal axes of the birefringent material are inclined at an angle of 45° to the polarizer and analyzer, the wavelengths of the extinctions are given by the well-known equation,[13]

$$t\Delta n = m\lambda, \tag{1}$$

where t is the thickness of the birefringent specimen, Δn is the birefringence i.e. the difference between the extraordinary and ordinary indices, m is an integer and λ is the wavelength of light. Our experimental set-up consisted of a source of white light (tungsten filament lamp or sunlight reflected by a

mirror) sequentially followed by a condensing lens, a polarizer whose vibration direction was at 45° to the vertical, a nematic sample oriented such that the director was along the vertical direction, a microscope which focuses the enlarged image of the specimen on the slit of the spectrograph, an analyzer with its vibration direction perpendicular to that of the polarizer, and finally the spectrograph. Suitable apertures were introduced in the path of the beam in order to secure the depth of focus of the enlarged image formed on the slit of the spectrograph. In the experimental geometry used by us, the Williams domains are horizontal. Figure 2(b) exhibits the schematic arrangement of the experimental set-up.

The nematic compound PBPA was chosen for the studies described in the following, because (i) it was readily available, (ii) its birefringence had already been investigated by us[14] and (iii) it is nematic at ordinary temperatures. The above compound was from the same batch as the sample that was used by us in our birefringence studies and hence in the calculations to be described later in

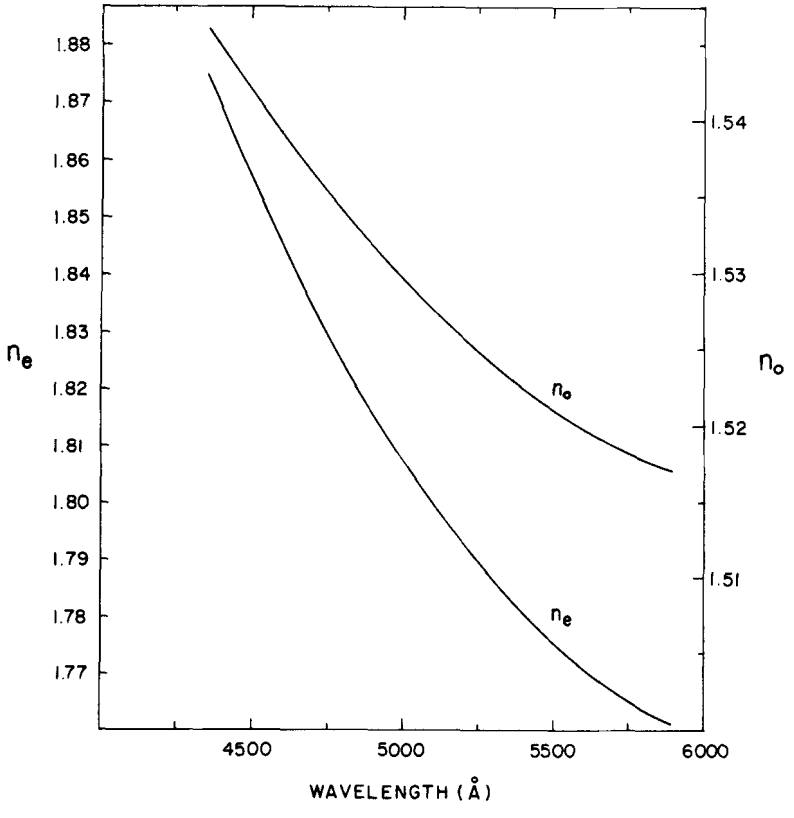

FIGURE 3 Dispersion of the refractive indices of PBPA at 27°C.

this paper we have used the same birefringence data. The chemical PBPA was obtained from M/s Eastman Organic Chemicals, USA, with a given purity of 98% *minimum* (by nonaqueous titration). The nematic-isotropic transition temperature determined by using the polarizing microscope was found to be 69.1°C in good agreement with the value of 69°C listed for this compound by M/s Eastman Organic Chemicals and Atomergic Chemetals, USA. The birefringence data for different wavelengths for this compound at the room temperature of 27°C (at which the present experiments were carried out) are shown graphically in Figure 3. The sample of PBPA used in the above experimental arrangement was sandwiched between a pair of tin oxide-coated transparent conducting glass plates, between which was applied a variable frequency alternating voltage from a suitable power supply. Cleaved mica was used as spacer. We did not make use of dc electric fields since alternating fields are preferable (see for example, Penz).[11] The specimen remained in the nematic phase in the supercooled state at room temperatures for a considerable length of time of about 12 hours, after which it crystallized into the solid. Therefore, care was taken to see that the experiments were completed before the onset of crystallization, which was marked by the turbidity commonly observed with polycrystalline solids.

3 THEORETICAL CONSIDERATIONS

The periodic distortion in the orientation of the director **S** in the presence of the applied electric field, as assumed by Penz,[11] is given by the following equation

$$\mathbf{S} = \hat{e}_1 + \left[\theta_0 \cos(qx_1)\cos\left(\frac{\pi x_2}{t}\right)\right]\hat{e}_2. \tag{2}$$

In the above, the unit vector $\hat{e}_1$ corresponds to the direction of **S** in the absence of the electric field, (i.e. the rubbing direction) and unit vector $\hat{e}_2$ corresponds to the direction of propagation of the light wave, [see Figure 2(a)]. Here, we make use of an orthogonal coordinate system $\hat{e}_1$, $\hat{e}_2$, and $\hat{e}_3$ with the corresponding coordinates x_1, x_2, and x_3. The factor $\cos(\pi x_2/t)$ in Eq. (2) was introduced by Penz to ensure the fact that the molecules at the surface boundaries of the pair of conducting glass plates ($x_2 = \pm t/2$) have not suffered any change in their orientation. In Eq. (2), q corresponds to $2\pi/L$, where L is equal to twice the spacing between the stripes. Here, θ_0 may be interpreted as the amplitude of distortion.

In the absence of the applied field, for the propagation of light along $\hat{e}_2$, the two refractive indices associated with the oriented nematic medium are the extraordinary and ordinary indices n_e and n_0. The former corresponds to the

case of the incident electric vector being along $\hat{e}_1$ and the latter to the case for which the electric vector is along $\hat{e}_3$. When the external electric field is applied, the local direction of **S** is given by the Eq. (2), and **S** is always perpendicular to $\hat{e}_3$ and hence the ordinary index is independent of x_1 and x_2, and shall be denoted hereafter by n_0. If β is the angle made by **S** with $\hat{e}_2$ [vide, Figure 2(a)] the extraordinary refractive index n'_e for light vibrations along $\hat{e}_1$ is given by the well-known relation,

$$(n'_e)^2 = n_e^2 n_0^2 (n_e^2 \cos^2 \beta + n_0^2 \sin^2 \beta)^{-1}. \tag{3}$$

Here, $\beta = (\pi/2 - \theta)$, where θ is the angle between **S** and $\hat{e}_1$. For small values of θ it may be shown easily that the extraordinary index n'_e is given by,

$$n'_e = n_e \left[1 - \frac{\theta^2 (n_e^2 - n_0^2)}{2n_0^2} \right]. \tag{4}$$

Further, for small values of θ, it may also be shown that θ is given by,

$$\theta = \theta_0 \cos(qx_1) \cos\left(\frac{\pi x_2}{t}\right). \tag{5}$$

Therefore, when light is polarized along $\hat{e}_1$ and is propagating through the nematic medium along $\hat{e}_2$, the total optical path described by it is given by,

$$\int_{-t/2}^{+t/2} n'_e \, dx_2 = t n_e - \frac{t n_e \theta_0^2}{4n_0^2} (n_e^2 - n_0^2) \cos^2(qx_1). \tag{6}$$

It may be pointed out here that the expression used by Penz[11] for n'_e in the integral given above is found to be inappropriate, because his approximate expression for n'_e corresponds to the case where the value of θ lies close to $\pi/2$, instead of the actual case here of θ being small.

4 RESULTS AND DISCUSSION

The path difference between the extraordinary and ordinary waves immediately on emergence through the thin layer of the specimen of thickness t is given by,

$$\int_{-t/2}^{+t/2} n'_e \, dx_2 - t n_0. \tag{7}$$

When no electric field is applied to the conducting glass plates, $\theta_0 = 0$ and there is no variation in the extraordinary index n_e with x_1 and x_2 and $n'_e = n_e$ corresponding to the maximum value of the extraordinary index of the homogeneously oriented specimen. When the magnified image of the specimen

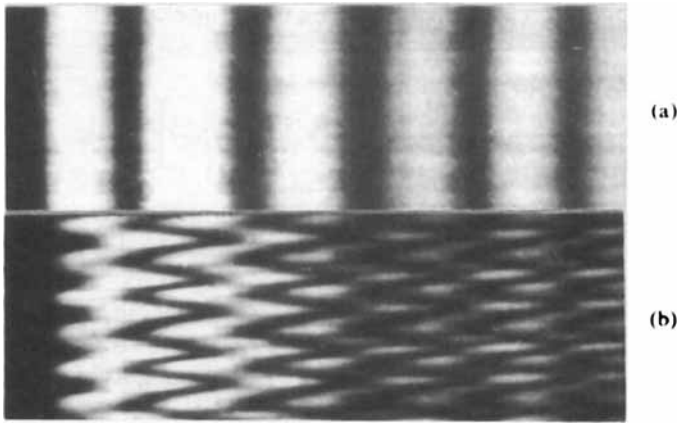

FIGURE 4 (a) Banded spectrum observed with the specimen between crossed polars, when no electric field was applied. (b) Banded spectrum of vertical sinusoidal bands observed with the same specimen to which an alternating voltage of 21.9 V, (975 Hz) is applied. Thickness of specimen was 18.45 μm.

is focused on the slit of the spectrograph (as described earlier above), associated with every point on the object plane of the specimen there is a corresponding point on the image plane. The relative path difference which arises between the extraordinary and ordinary waves (emerging from any point on the object plane) will be preserved when the waves reach the corresponding point on the image plane. This path difference is (i) a function of the wavelength of light and (ii) a function of x_1, or in other words is a function of x_1' in the image plane, x_1' being equal to Mx_1, where M is the magnification factor. Correspondingly on the image plane the variation of θ with x_1 and x_2 will be given by the expression,

$$\theta = \theta_0 \cos(q'x_1')\cos\left(\frac{\pi x_2}{t}\right). \tag{8}$$

Here, $q' = 2\pi/L'$ and L' is equal to twice the spacing of the stripes in the image plane, and given by $L' = ML$. Evidently, we have $q'x_1' = qx_1$.

For the experimental arrangement described in Section 2, in the absence of the electric field, the wavelengths of extinction in the spectrum of the transmitted light will be given by,

$$t(n_e - n_0) = m\lambda, \tag{9}$$

m being an integer. In the absence of the field, therefore it emerges that the spectrum exhibits a series of extinctions at different wavelengths as shown in Figure 4(a).

The corresponding equation for the case when the electric field is applied is given by,

$$t\left[(n_e - n_0) - \frac{\theta_0^2 n_e}{4n_0^2}(n_e^2 - n_0^2)\cos^2(q'x_1')\right] = m\lambda, \tag{10}$$

m being an integer. In the presence of the field the extinctions change over from straight vertical bands to vertical sinusoidal bands. The different sinusoidal bands start out from a wavelength corresponding to those of the straight bands and make excursions towards the short wavelength side and back to the wavelength corresponding to that of the respective straight bands. The above features are exhibited in Figure 4(b). The wavelengths of the maximum excursion (towards the short wavelength side) for the different bands are obtained by putting $\cos^2(q'x_1') = 1$ in Eq. (10). For a given m, let λ_1 and λ_2 be the wavelengths of the long wavelength and short wavelength edges of the excursions of sinusoidal bands. λ_1 and λ_2 are given by,

$$t(n_e - n_0) = m\lambda_1, \tag{11}$$

and

$$t\left[(n_e - n_0) - \frac{\theta_0^2 n_e}{4n_0^2}(n_e^2 - n_0^2)\right] = m\lambda_2. \tag{12}$$

All the refractive indices appearing on the left hand side of the Eq. (11) and Eq. (12) refer respectively to their values appropriate to the wavelengths λ_1 and λ_2. By dividing Eq. (12) by Eq. (11), t and m may be eliminated, and θ_0 may be calculated readily from measurements of the values λ_1 and λ_2 for the different bands, and using the values of n_e and n_0 at the required wavelengths from our data shown graphically in Figure 3. The values of m and hence t also may be obtained by plotting on separate strips of graph paper $[\log(n_e - n_0)_{\lambda_1} - \log \lambda_1]$ and $\log m$ and matching these two strips. In our experiments the values of t, were in the range of 10 to 50 μm.

• The values of θ_0 thus calculated from measurements made on the different bands are found to agree very well, as may be seen from the three representative sets of values shown in Table I for alternating fields of different voltages and frequencies. In the case of PAA the value of θ_0 was estimated by Penz[11] to be around 18° from his measurements on the focal lengths of the series of cylindrical lenses associated with the Williams domains. It is found from our experiments that for a given frequency, the values of θ_0 increase with increasing voltage, the variation being practically linear as shown in Figure 5. That the distortion increases with increasing voltage is well-known and in

TABLE I

Wavelengths of the interference minima and the amplitudes of periodic distortion

Frequency voltage and thickness t	order m	λ_1 in Å	λ_2 in Å	$(n_e - n_0)\lambda_1$	$(n_e - n_0)\lambda_2$	θ_0 in degrees
	8	5720	5490	0.248	0.255	18.6
500 Hz	9	5340	5150	0.261	0.269	18.2
13.25 V	10	5060	4890	0.275	0.285	18.5
$t = 18.45$ μm	11	4840	4680	0.288	0.299	18.5
	12	4650	4510	0.302	0.314	18.2
	18	5725	5470	0.247	0.256	20.1
	19	5560	5290	0.253	0.263	20.9
600 Hz						
14.25 V	20	5405	5150	0.259	0.269	20.6
$t = 41.66$ μm	21	5255	5040	0.264	0.276	20.5
	22	5125	4920	0.271	0.283	20.2
	23	5010	4810	0.277	0.289	20.1
	8	5720	5410	0.248	0.258	21.7
700 Hz	9	5340	5090	0.261	0.273	21.3
16.5 V	10	5060	4830	0.275	0.289	21.3
$t = 18.45$ μm	11	4840	4630	0.288	0.304	21.5

λ_1 corresponds to the longer wavelength edge and λ_2 corresponds to the shorter wavelength edge of the sinusoidal bands, and are accurate to within ± 10 Å only, owing to the considerable width of the dark bands.

fact the Williams domain pattern collapses when the applied voltages are sufficiently high, owing to the onset of turbulence (see e.g. de Gennes).[3]

5 SOME FURTHER OPTICAL OBSERVATIONS

The periodic nature of the variation of the distortion was also confirmed by us by using a Babinet compensator and an experimental set-up exactly identical to that used in our studies on ringed spherulites.[12] The details of the experimental arrangement are fully described in that paper. An enlarged image of the specimen was focused (with the aid of a microscope) on the plane of the Babinet compensator, the orientation of the specimen being such that the Williams domains were horizontal. The observations were made between crossed polars as usual. When no electric field was applied, vertical straight bands are observed and these bands transform to vertical sinusoidal bands when the electric field is applied. These features are exhibited in Figure 6.

In the following, we give a brief explanation of the above features. When the specimen and the Babinet compensator are between crossed polars, (the

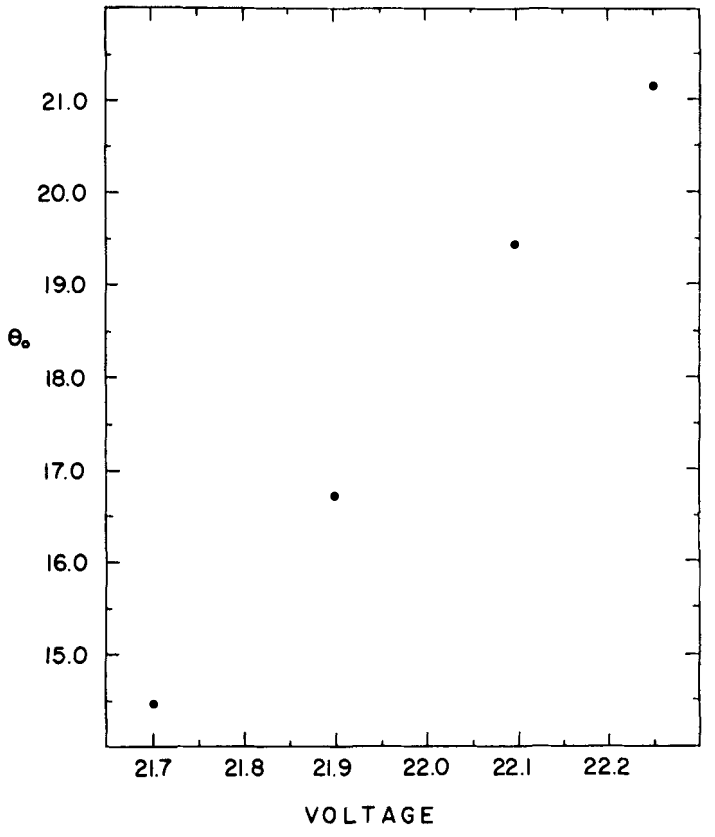

FIGURE 5 Variation of θ_0 with the applied alternating voltage at a frequency of 975 Hz.

vibration directions of the crossed polars being at 45 and 135° to the vertical) the interference minima are given by the condition that,

$$\delta_1 + \delta_2 = 2m\pi, \tag{13}$$

where m is an integer and δ_1 and δ_2 are the phase differences arising between the vertical and horizontal components of vibration during their passage through the nematic medium and the Babinet compensator respectively. From Eq. (10), δ_1 may be seen to be given by,

$$\delta_1 = \frac{2\pi t}{\lambda}\left[(n_e - n_0) - \frac{\theta_0^2 n_e}{4n_0^2}(n_e^2 - n_0^2)\cos^2(q'x_1')\right]. \tag{14}$$

δ_2 is given by,

$$\delta_2 = \frac{2\pi s}{s_0}, \tag{15}$$

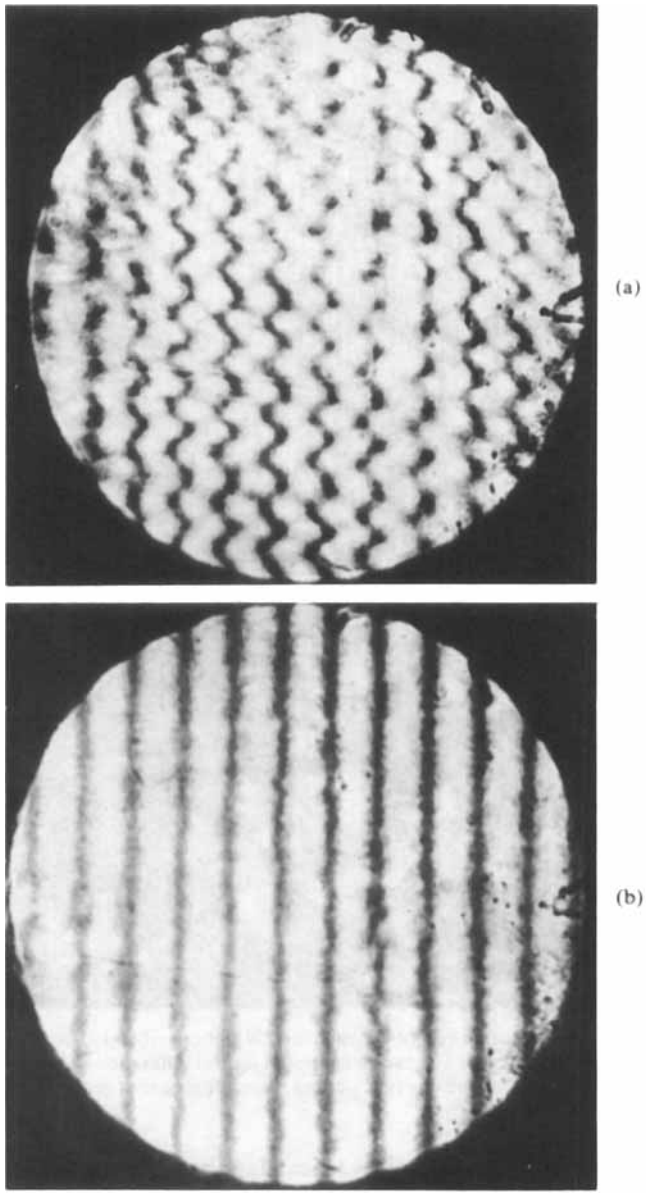

FIGURE 6 Interference pattern observed when the specimen ($t = 18.45\ \mu m$) and the Babinet compensator were kept between crossed polars. A red filter was used in the path of the incident beam of sunlight. (a) The vertical sinusoidal dark bands observed with the same specimen to which an alternating voltage of 21.9 V, (975 Hz) is applied. (b) The vertical dark bands in the absence of the field.

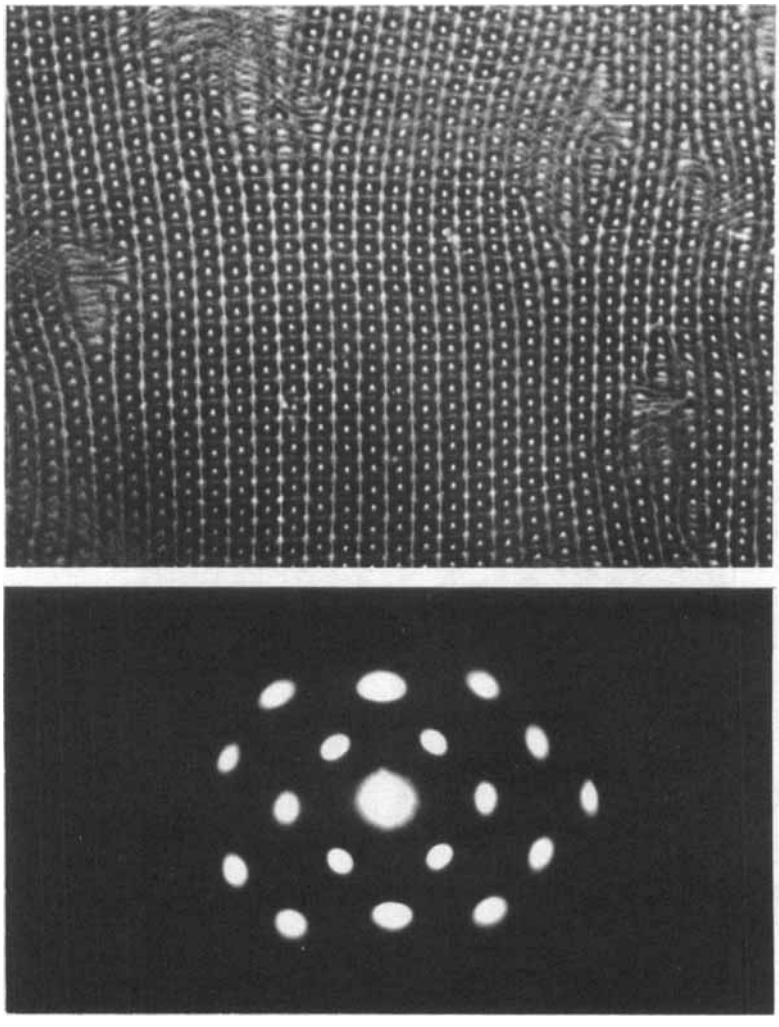

FIGURE 7 (a) Microphotograph of a dynamic grid pattern obtained with a specimen of PBPA (t = 13.63 μm) 235 x. (b) The two dimensional optical diffraction pattern obtained with the specimen exhibiting the above dynamic pattern, using unpolarized red light.

where s_0 is the spacing between the vertical dark bands observed in the field of view of the Babinet compensator when monochromatic light is used. s is the horizontal distance of any point (for which δ_2 is required) from the central achromatic dark band ($m = 0$) observed with white light. It is readily shown from Eq. (14) and Eq. (15) that the amplitude of distortion θ_0 is related to Δs, the excursion from right to left of any particular sinusoidal band (i.e., of any

given m). This relation is given by,

$$\frac{\Delta s}{s_0} = \frac{t}{\lambda}\left[\frac{\theta_0^2 n_e}{4n_0^2}(n_e^2 - n_0^2)\right]. \tag{16}$$

The measurements were carried out with the sinusoidal bands observed, using an alternating voltage of 14.25 V, (600 Hz) and with incident radiation of wavelength 5893 Å. The thickness of the specimen was 41.66 μm. From the known values of n_e and n_0, and the measured values of Δs ($= 0.14$ cm) and s_0($= 0.104$ cm), the value of θ_0 was calculated to be 20.2°. This value is in agreement with the values of θ_0 given in Table I for the specimen of the same thickness and at the same voltage and frequency. Similar agreement is obtained for other alternating voltages and frequencies.

It is found that at the higher voltages the domain pattern is transformed into a two dimensional network (i.e., a dynamical grid pattern) as shown in Figure 7(a). For example, this pattern is observed when an alternating field of frequency 600 Hz and a voltage of about 20 volts is applied to the specimen sandwiched between conducting glass plates. The average dimension of each grid is 16 μm × 11 μm. Similar patterns have been reported by Kai *et al.*[15] and Weir and Gelerinter,[16] in the case of other compounds. That the grid pattern corresponds to a two dimensional periodic distortion, is confirmed from the two dimensional optical diffraction pattern observable with the specimen and shown in Figure 7(b). Such patterns have been reported by other investigators also.[17–20] The diffraction pattern shown in Figure 7(b) is reminiscent of the diffraction pattern which one obtains with crossed diffraction gratings.

Acknowledgement

The authors are thankful to the University Grants Commission (India) for the research grant provided for the project on liquid crystals. One of us (DR) wishes to express his thanks to the University Grants Commission (India) for the award of a Junior Research Fellowship, and to the CSIR (India) for the award of a Senior Research Fellowship.

References

1. R. Williams, *J. Chem. Phys.*, **39**, 384 (1963).
2. N. V. Madhusudana, P. P. Karat, and S. Chandrasekhar, *Curr. Sci.*, **42**, 147 (1973).
3. P. G. de Gennes, *The Physics of Liquid Crystals* (Clarendon Press, Oxford, 1974), p. 192.
4. P. P. Karat and N. V. Madhusudana, *Pramana, Suppl.* **1**, 285 (1975).
5. K. Hirakawa and S. Kai, *Mol. Cryst. Liq. Cryst.*, **40**, 261 (1977).
6. S. Lu and D. Jones, *J. Appl. Phys.*, **42**, 2138 (1971).
7. L. K. Vistin, S. V. Rychkova, and N. M. Malikova, *III All Union Conf. Liq. Cryst. and Pract. Applic.* (Ivanovo, 1974).
8. I. D. Samodurova and A. S. Sonin, *III All Union Conf. Liq. Cryst. and Pract. Applic.* (Ivanovo, 1974).

9. H. Tsuchiya and K. Nakamura, *Mol. Cryst. Liq. Cryst.*, **29**, 89 (1974).
10. A. Takase, S. Sakagami, and M. Nakamizo, *Jap. J. Appl. Phys.*, **14**, 228 (1975).
11. P. A. Penz, *Phys. Rev. Lett.*, **24**, 1405 (1970).
12. D. Krishnamurti, M. S. Madhava, and D. Revannasiddaiah, *Mol. Cryst. Liq. Cryst.*, **47**, 155 (1978).
13. W. A. Wooster and A. Breton, *Experimental Crystal Physics* (Clarendon Press, 1970), p. 13.
14. D. Revannasiddaiah and D. Krishnamurti, *Mol. Cryst. Liq. Cryst.*, (In press). 1979.
15. S. Kai, K. Yamaguchi and K. Hirakawa, *Jap. J. Appl. Phys.*, **14**, 1385 (1975).
16. R. C. Weir and E. Gelerinter, *Mol. Cryst. Liq. Cryst.*, **40**, 199 (1977).
17. C. Deutsch and P. N. Keating, *J. Appl. Phys.*, **40**, 4049 (1969).
18. E. W. Aslaksen and B. Ineichen, *J. Appl. Phys.*, **42**, 882 (1971).
19. G. Assouline, A. Dmitrieff, M. Harneg, and E. Leiba, *J. Appl. Phys.*, **42**, 2567 (1971).
20. A. Takase, S. Sakagami, and Nakamizo, *Jap. J. Appl. Phys.*, **12**, 1255 (1973).